

RF Generation using Nonlinear Transmission Lines for Aerospace Applications

Fernanda S. Yamasaki¹, José O. Rossi, Joaquim J. Barroso

Associated Plasma Laboratory
National Institute for Space Research
São José dos Campos, Brazil
fernandayamasaki@hotmail.com¹

Abstract — As an alternative to replace microwave tubes used nowadays in compact space systems for satellites communications, this work examines the feasibility of using nonlinear transmission lines (NLTL) consisting of nonlinear components as varactor diodes, or capacitors modeled nonlinearly, as ideal circuits, without ohmic losses and real ones, with ohmic losses. All simulations were confirmed using equations found in the literature to verify the models validity. It was also verified that high voltages prevent the use of varactor diodes in NLTLs. This makes the selection for ceramic capacitors more suitable in such applications.

Keywords— varactor diode; ceramic capacitor; nonlinear component; RF generation; soliton.

I. INTRODUCTION

Motivated by two scientific works, there has been a great interest in the study of nonlinear transmission lines (NLTLs) for high power RF generation. The first one [1], a ferrite NLTL produced 20 MW RF peak power with 20% efficiency at 1.0 GHz. The second one [2], a ceramic capacitive NLTL provided 60 MW RF power peak in the 100–200 MHz range. However, line dielectric losses in the ceramic limited the output frequencies below 200 MHz [3]. To deal with this problem other works [4]–[6] have studied the operation of these lines using numerical programs as NLTL closed-form solutions cannot be derived to predict the exact equation for an input rectangular pump pulse. Line properties corresponding to the characteristics of soliton formation (nonlinearity and dispersion) acting in combination permit the occurrence of high frequency oscillations along the line, which can be used to feed a load through an RF antenna matched to the line output. Therefore, the aim of this work is to study the behavior of these nonlinear components, in special variable capacitance diodes or ceramic capacitors, by using Spice circuit simulations and comparing them to experimental results for model validation.

II. NLTL OPERATION THEORY

When an input pulse is injected into a dispersive lumped LC line it propagates down along the line length with a velocity given by $c = 1 / (LC)^{1/2}$. If the line is nonlinear with

Work supported by SOAR – USAF under contract number FA9550-13-0132.

variable capacitance as shown in Fig.1 the portion of the pulse with higher amplitude will travel faster than its lower initial amplitude as C decreases with increasing voltage. In this way, the pulse peak catches up with the low voltage amplitude, forming an output shock wave front with a very fast rise time. However, as the line is dispersive the output shortest rise time will be limited by the Bragg cutoff frequency:

$$f_{c0} = 1 / \pi \sqrt{LC(V_{max})} \quad (1)$$

where C (Vmax) is the decreased capacitance at the maximum voltage applied.

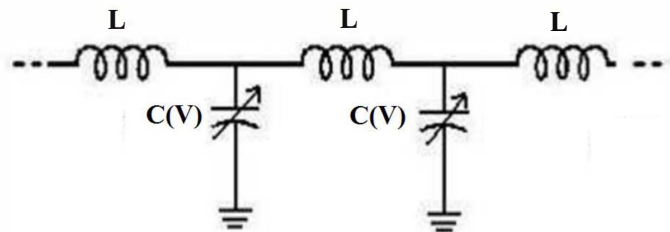


Fig. 1. A section of a capacitive nonlinear line.

One way to understand how soliton oscillations are produced in these lines is shown in Fig. 2. Assuming that a trapezoidal pulse is injected into the line input and the portion of the rise time is approximated by a series of small rectangular pulses with increasing amplitudes and decreasing widths, then each narrow rectangular pulse injected into a nonlinear line generates a soliton that propagates down the line, so that their areas are equally conserved [7,8]. Solitons can be represented by a squared hyperbolic function, whose amplitude increases with their propagation velocity while the inverse phenomenon is observed for the width. Thus, solitons of higher amplitudes have higher velocities than those of lower amplitudes and they arrive first at the line output. This generates a series of solitons with decreasing amplitudes at the output as shown in Fig. 2.

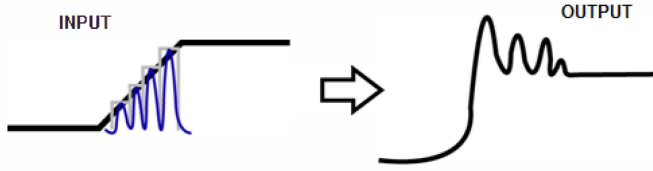


Fig.2 Soliton generation produced in a NLTL.

A rough estimate for the pulse rise time reduction caused by the LC ladder sections is made by calculating the time delay difference between the lower amplitude portion and the peak of the propagating pulse as [9]:

$$\Delta T = t_{ri} - t_{ro} = n(\sqrt{LC_0} - \sqrt{LC(V_{max})}) \quad (2)$$

where t_{ri} is the input rise time, t_{ro} is the output rise time, n is the number of sections of the line and C_0 is the unbiased capacitance.

The pulse rise time reduction is limited ultimately by the lower cutoff frequency of the LC ladder as the propagating pulse cannot be submitted to further sharpening if n tends to a high number and, consequently the spectrum of frequencies from the shock wave is separated since the energy cannot propagate above f_{c0} , producing at the output a series of narrow pulses (solitary waves) of high frequency on the order of f_{c0} . Therefore, (2) becomes:

$$\Delta T = n(1 - \sqrt{k})\sqrt{LC_0} \approx \pi \sqrt{LC(V_{max})} = \pi \sqrt{k}\sqrt{LC_0} \quad (3)$$

where the nonlinearity factor $k = C(V_{max})/C_0$. Canceling $\sqrt{LC_0}$ on both sides and isolating k obtains:

$$k = \left(\frac{n}{n + \pi}\right)^2 \quad (4)$$

It is noted in (4) that for a large value of n , $C(V_{max})$ is slightly below the value of C_0 , indicating that for a large number of sections n the nonlinearity factor k can be very close to unity, which means that capacitors with more stable capacitance can be used. This explains why in practice it is easier to produce a sufficient number of oscillations (i.e. a train of solitons) with reasonable amplitude output when a NLTL is built with 50 or more sections.

III. NONLINEAR CAPACITIVE DEVICES MODELING

First of all, to study the behavior of the capacitive NLTLs, it is important to model the capacitance variation of the nonlinear device ($C \times V$). Normally for low power NLTLs diodes with variable capacitance, known as varactors, are used. The width of reverse depletion zone of the varactors increases with the applied voltage and, thus the associated capacitance C varies inversely with the applied voltage V [10] as:

$$C(V) = \frac{C_{j0}}{\left(1 + \frac{V}{V_j}\right)^m} \quad (5)$$

where V_j is the junction potential, V is the applied voltage and C_{j0} is the unbiased junction capacitance.

In general, for applications in high power NLTLs varactors are not suitable because of their small reverse breakdown voltage and low current rate. Then in these applications, ceramic capacitors are more appropriate, and therefore, their characterization and the subsequent implementation of corresponding the $C \times V$ models in Spice programs are of great importance for the NLTL design. Normally, capacitance of nonlinear ceramic capacitors decreases with the voltage, but for some capacitors as the PMN there is an initial alignment of the dipoles before reaching saturation, which means an initial increase of C with voltage before reaching the saturation peak. A generic model to represent the $C \times V$ variation is based on Gaussian curve type named Lorentzian [11] as shown in Fig. 3.

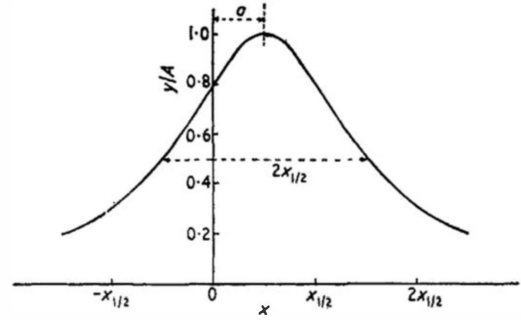


Fig. 3 - Normalized Lorentzian function, where A is the amplitude peak and $x_{1/2}$ is half the full width at the maximum height [12].

The $C \times V$ curve obtained from the manufacturer is shown in Fig. 4 by dotted line, where the fitting by the Lorentzian function is represented by the blue line. The corresponding mathematic formulation for the capacitance as function of the voltage $C(V)$ is given below:

$$C(V) = \frac{C_0 V_{HWFM}^2}{V_{HWFM}^2 + (V - V_0)^2} \quad (6)$$

where $V_{HWFM} = 4500$ V is the half of the full voltage width at the peak amplitude of C ; $C_0 = 270$ pF is the peak capacitance at the potential $V_0 = 4000$ V.

Other formulation for the Lorentzian curve based on a hyperbolic tangent function was also proposed elsewhere [13]. This new fitting with the experimental data provided by the maker is given by the red line in Fig. 4 and the corresponding mathematical formulation is given below.

$$C(V) = (C_0 - C_{sat}) \cdot \left[1 - \tanh^2\left(\frac{V - V_0}{V_{sat}}\right)\right] + C_{sat} \quad (7)$$

IV. RESULTS

where C is the final capacitance at the applied voltage, $C_0 = 270$ pF is the peak capacitance at $V_0 = 4$ kV, $C_{sat} = 20$ pF is the capacitance on saturation, and $V_{sat} = 5$ kV is the voltage at which saturation begins to take place.

As can be seen from the comparison between both curves (in Fig. 4) there is a good agreement, which shows that both proposed formulations can be used for modeling capacitive NLTLs made of ceramic capacitors.

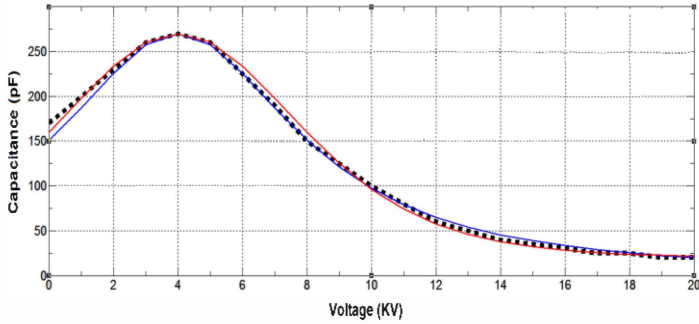


Fig. 4 - Comparison of the $C \times V$ curves for capacitor PMN38: experimental (black); Lorentzian function (in blue) and hyperbolic function (in red).

Spice circuit simulators (such as Circuit Maker, Microcap, etc) are normally used to simulate NLTLs built with varactor diodes as they have models in their library that represent these devices with variable capacitance. However, when the NLTL is built with ceramic capacitors, the great majority of these softwares are not suitable because they do not have models for variable capacitors, with the exception of the LT-Spice program. Thus, for simulating lines with nonlinear ceramic capacitors LT is used exclusively. The LT-Spice enables the modeling of a variable capacitance by knowing the capacitor charge equation. This equation can be implemented directly through a command line in the capacitance value on the graphical simulator drawing.

Therefore the charge accumulated in the capacitor can be calculated as $\int C(V) dV$ and from (6) and (7) obtains respectively;

$$Q = C_0 * V_{HWF M} * \arctan \left[\frac{V - V_0}{V_{HWF M}} \right] \quad (8)$$

$$Q(V) = (C_0 - C_{sat}) V_{sat} \tanh \left(\frac{V}{V_{sat}} \right) + C_{sat} V \quad (9)$$

Both above equations can be used in LT to represent the PMN ceramic capacitor since we have shown that there is a good fitting between both formulations (see Fig. 4 again)

To test the validity of the models of variable capacitance devices, a varactor NLTL was built. The line was mounted on a phenolite PCB using 10 LC sections with commercial fixed inductors $L = 2.7$ μ H and the FMMV109 varactor as nonlinear capacitor. The Spice NLTL model also included ohmic losses of L and C (respectively, $R_L = 0.56$ Ω and $R_C = 6.8$ Ω). In (5) note that $C = C_{j0}$ for $m = 0$ as expected and generally in many cases $m = 1/2$. From the FMMV109 datasheet, C_{j0} and V_j are assumed to be respectively 61.30 pF and 0.70 V in simulations while m is the main varactor parameter to be investigated to produce a good fitting between experimental and simulations results. The line is fed by a 50 Ω output impedance pulse generator with 11 V_{output} amplitude pump pulse of 350 ns duration and 110 ns rise time as shown in Fig. 5 by the experimental result in red. As the input pulse rise time is greater than the rise time reduction factor ΔT (of the order of 80 ns with $m = 0.70$) the pulse is sharpened at the output as shown in Fig. 6 by the red line, in which it is noticed clearly that the output pulse rise time is reduced to approximately 30 ns. Figs. 5 and 6 also compare the corresponding Spice simulations and experimental results using two different circuit simulators (LT-Spice and Circuit Maker - CM). As an example, two different values of m ($= 0.36$ and 0.7) were used to run the simulations. In Fig. 6 it is observed good agreement between simulation and experiment for both values since in any case the 50 Ω generator output impedance is much less than the line impedance $Z = \sqrt{L/C(V_{max})}$. Nevertheless, a better fitting between results at output (shown in Fig. 6) is achieved with higher $m = 0.70$ as dispersion effect is much weaker than nonlinear effects in this case because of the longer input pulse rise time.

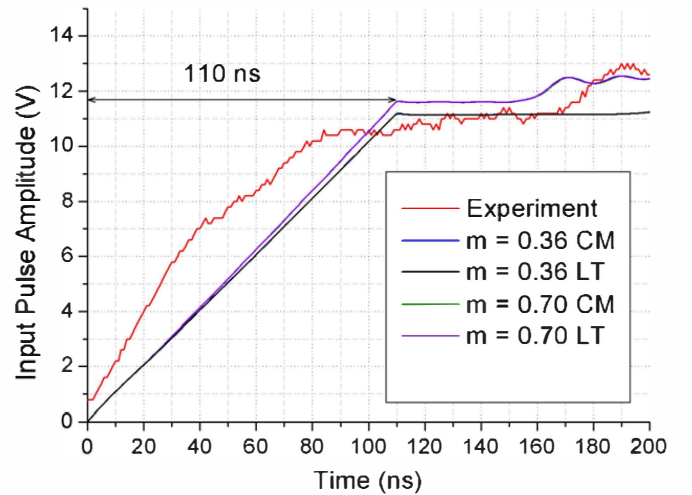


Fig. 5 - Pulse sharpening case: input pulse

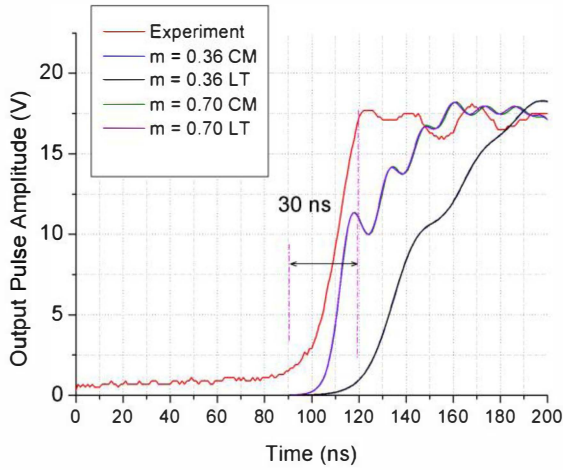


Fig. 6 - Pulse sharpening case: output pulse

On the other hand, using a pulse generator of lower rise time so that $t_{ri} < 30$ ns, factor ΔT is limited by line dispersion and, thus high frequency soliton-type oscillations appear on the output pulse amplitude as shown in Fig. 7. The best fitting between simulations and experimental curves were obtained using the same previous line parameters ($C_{j0} = 61.30$ pF e $V_j = 0.70$ V), but with reduced m ($= 0.36$) for a 10 V input pulse amplitude. Note in this case that the stronger dispersive effect tends to reduce the wave phase velocity, which in turn reduces the factor m . Moreover observe in results of Fig. 7 that f_{co} limits the output rise time to 25 ns approximately as expected and that oscillation frequency is on the order of 40 MHz. Finally, it is verified in all the results that equal responses are obtained using LT and CM circuit simulators.

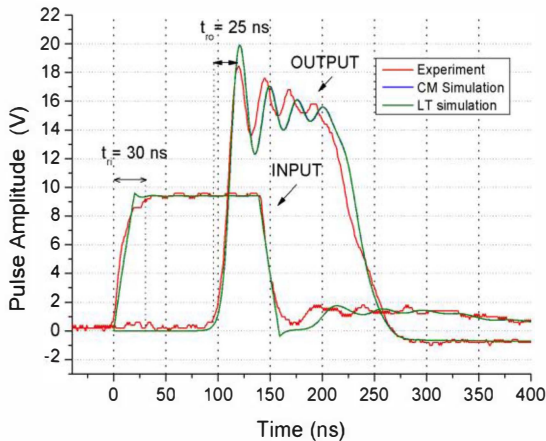


Fig. 7 - Input and output pulses for oscillatory case.

To test the ceramic capacitor in Spice simulator, it is assumed a lossless NLTL made of 170 pF PNM ceramic capacitors (see Fig. 3) and air core inductances of about 13 nH

with 50 sections. According to (1) in this case it is predicted a soliton generation of about 200 MHz considering $C(V_{max}) = 50$ pF. For this case, only LT Spice simulator was used since only this program has the capability of simulating a nonlinear variable capacitance in a simple way (just to the authors' knowledge) as explained in last section. Both models using ceramic capacitor represented by (8) and (9) were implemented in LT-Spice circuit simulations. Fig. 8 shows the respective simulations for the PMN NLTL using both models given by (8) and (9) at a high power level fed by a pulse generator of 16 kV with output impedance of 6 ohms, pulse rise time of about 5 ns, and width of 40 ns. The simulated line has a characteristic impedance of approximately 16 ohms for the maximum applied voltage. In Fig. 8 it can be noticed that there is a good agreement between both models, which confirms the validity of the models used in Spice simulation.

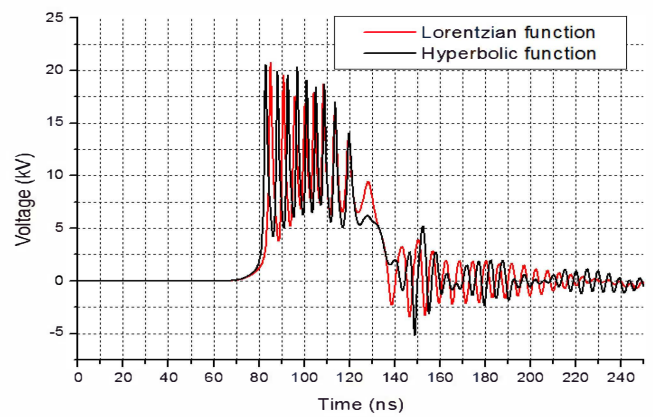


Fig. 8 – NLTL output pulse obtained for both models.

In addition as shown in Fig. 9, the fast Fourier transform of the output voltage is traced in this case by the simulator to confirm that the soliton generation corresponds to a frequency of the order of 200 MHz as expected. This is confirmed in this figure observing that the amplitudes of harmonics with frequencies above 200 MHz are negligible.

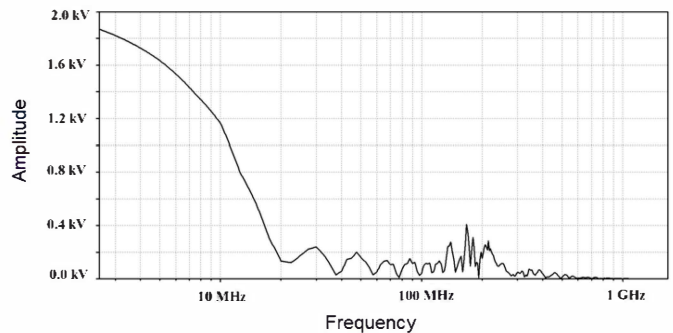


Fig. 9 – FFT of the output pulse simulated for PMN NLTL.

V. CONCLUSIONS

In this paper, it was shown that NLTLs can be used for pulse sharpening or RF generation depending on the rise time of the input pulse applied. Also circuit models developed have been validated by means of Spice simulations. In particular, for the case of a low voltage/power NLTL simulations and experimental data were compared using a varactor NLTL prototype. However, in this case the small discrepancies observed between the results are probably due to two main factors: a) 10 % variation of the parameter C_{j0} of the varactors used in the NLTL (according their data sheet specification) and b) input pulse approximation by a slow ramp in Spice simulation rather than a convex curve as seen in the respective experimental curves (Figs. 5 and 6).

For high power NLTLs, ceramic capacitors must be employed because of their higher nominal voltage. The modeling of $C \times V$ curves of ceramic capacitors for use in NLTLs proved to be feasible in Spice simulation as a powerful tool for the design of NLTLs. Although the simulations could not be compared to experimental results using a prototype due to the higher voltages involved, the both models proposed for these nonlinear devices showed good results in terms of simulations Spice, which is according to what is expected from the design of a lossless 200 MHz NLTL. Finally, the LT-Spice program has revealed to be a good circuit simulator for NLTLs because of its capability of modeling nonlinear components.

VI. REFERENCES

- [1] B. Seddon, C. R. Spikings, and J. E. Dolan, "RF pulse formation in NLTLs," in Proc. of the IEEE 16th International Pulsed Power Conf. (Albuquerque NM, 2007), pp.678-681.
- [2] P. M. Brown and P.W. Smith, "High power, pulsed soliton generation at audio & microwave frequencies", in Proc. of the 11th International Pulsed Power Conf.(Baltimore MD, 1997) pp. 346-354.
- [3] P. W. Smith, "Pulsed, high Power, RF generation from nonlinear dielectric ladder networks – performance limits," in Proc. of the 18th IEEE Int. Pulsed Power Conf. (Chicago, IL, 2011), pp. 167-172.
- [4] J. D. Darling and P. W. Smith, "High power RF generation from nonlinear delay lines," in Proc. of the 16th Int. Pulsed Power Conf., (Albuquerque NM, 2007), pp. 472-475.
- [5] J. O. Rossi and P. N. Rizzo, "Study of hybrid nonlinear lines for high power RF generation", in Proc. of the 17th IEEE Pulsed Power Conf., (Washington, DC, 2009) pp. 46-50.
- [6] N. S. Kuek, A. C. Liew, E. Schamiloglu, and J. O. Rossi, "Circuit modeling of nonlinear lumped element transmission lines including hybrid RF lines," IEEE Trans. on Plasma Science, vol 40, n.10, pp. 2523-2534, 2012.
- [7] R. Hirota, and K Suzuki, "Theoretical and experimental studies of lattice solitons in nonlinear lumped networks," in the Proceedings of the IEEE, v.61, n.10, Oct. p. 1483 – 1491, 1973.
- [8] K. Lonngren and A. Scott. Solitons in action. New York: Academic Press, 1978, p. 133.
- [9] P. W. Smith, Transient electronics – Pulsed circuit technology. John Wiley & Sons, West Sussex, England, 2002, pp. 245-249.
- [10] A.B. Kozyrev and D.W. Van Der Weide, "Nonlinear wave propagation phenomena in left-handed transmission line media," IEEE Transactions on microwave theory and techniques, v. 53., n. 1, p. 238-245, 2005.
- [11] D.M. French, B.W. Hoff, S. Heidger, and D. Shiffler, "Dielectric nonlinear transmission line," in Proc. of the 18th IEEE International Pulsed Power Conference, (Chicago IL, 2011) pp. 341-345.
- [12] W. Gough, "The graphical analysis of a Lorentzian function and a differentiated Lorentzian function," Journal of Physics, v. 1, n. 2, 1968.
- [13] N.S. Kuek, A.C. Liew, E. Schamiloglu, and J.O. Rossi, "Oscillating pulse generator based on a nonlinear capacitive transmission line," Accepted for publication in the IEEE Transactions on Dielectrics and Electrical Insulation, Oct. 2013.